ISBN: 978-3-95450-184-7 doi:10.18429/JACoW-IPAC2018-TUPAL064

EXTENDED-DOMAIN TUNE-SCANS FOR THE HL-LHC DYNAMIC APERTURE IN PRESENCE OF BEAM-BEAM EFFECTS *

D. Kaltchev, TRIUMF, Vancouver, Canada
D. Pellegrini, N. Karastathis, Y. Papaphilippou, E. McIntosh, CERN, Geneva, Switzerland

Abstract

Simulations of the HL-LHC dynamic aperture (DA) at collision energy and in the presence of beam-beam effects (weak-strong approximation) have been performed to determine the dependence of DA on the working point in tune space. Both linear domains of working points are explored and two-dimensional ones which focus on more promising sub-regions near the diagonal. The range of parameters, such as bunch intensity and emittance correspond to important HL-LHC scenarios.

In this work, the necessary resources were provided by the LHC@home project, based on the BOINC-SixTrack platform for distributed Computing.

INTRODUCTION

We report tune-scans – dependencies of the dynamic aperture of the HL-LHC [1] on the working point in tune space, covering both one-dimensional (linear) and two-dimensional tune domains. This study is a part of the detailed tracking campaign [2], [3] aimed at luminosity optimization and identification of operational scenarios for the HL-LHC. It employs the same standard tools [4], but focuses on somewhat extended tune domains of alternative shapes, features an independent procedure for generating initial conditions and processing the results and, most notably, emphasizes on the relation between dynamic aperture and resonances.

In the next section, linear tune-scans are described are – a continuation of previous studies for the LHC [5] and also natural development of fixed working point studies, e.g. [6], [7]. Considering resonances of very high order (16th) is found important to explain the observed (in tracking) reduction of DA near the nominal working point.

The last section describes results of two-dimensional scans which agree well with the findings in [2], [3].

At the end, a working point alternative to the one of the nominal HL-LHC is identified – of possible interest for future studies.

TUNE-SCAN (TS) PROCEDURE

We use latest Mad-X–SixTrack environment [4], [8], [9], [10] and HL-LHC lattices at collision energy with included weak-strong beam-beam interactions, sextupoles and Landau octupoles [11]. While DA is (traditionally) determined over 10^6 turns, short-term SixTrack runs for detuning with amplitude are often made in parallel (the footprint shown on Figure 1, left).

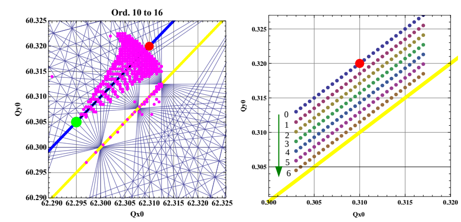

Figure 1: Tune-scan domains: linear (left) and 2D (right).

Setting the tune is illustrated on Fig. 1. The linearly perturbed beam-beam tune point $Q^{BB}_{x,y} = Q^0_{x,y} - \Delta Q^{BB}_{x,y}$ (green dot) is varied along the blue line parallel to the diagonal (left), or over a two-dimensional region made of many shifted such lines (right). All arc trim quadrupoles are used resulting in negligible mismatch [1]. By adding the exact tune-shifts $\Delta Q^{BB}_{x,y}$ for the particular lattice, all results will be presented in terms of the unperturbed working point (WP) $Q^0_{x,y}$. The minimum steps used, providing best resolution, were $\Delta Q^{\|\mathrm{diag.}} = 5\ 10^{-4}$and $\Delta Q^{\perp\mathrm{diag.}} = \sqrt{2}\ 10^{-3}$, however some 2D scans below employ 3-5 times larger step.

LINEAR TUNE SCANS

In this section, $Q^{BB}_{x,y}$ are constrained along line parallel to the diagonal: Fig. 1, left, and the LHC and HL-LHC lattices are taken at low chromaticity $\boldsymbol{Q'} \sim 2$-3 and without Landau octupoles ($\boldsymbol{I_{\mathrm{MO}}} = 0$).

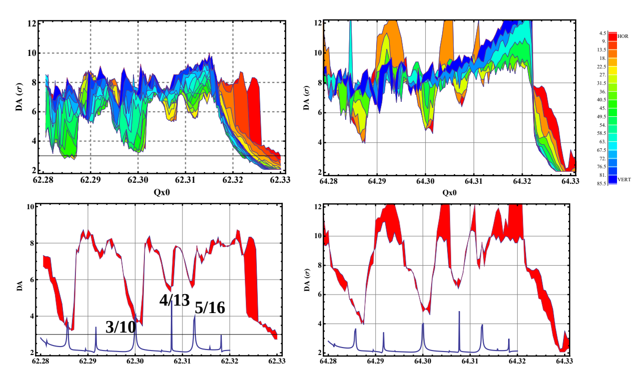

Figure 2: **Top two:** DA-by-angle curves for the case of HL-LHC (left) and LHC as built (right). **Bottom two:** Horizontal plane only (red) and Lie-theory prediction for dip locations (blue peaks).

We find that under these conditions both LHC and HL-LHC appear to be very near optimum tunes for several scenarios – see below the three cases in Table 1 – and, secondly, 16-th order resonances appear to be important near

* TRIUMF receives funding via a contribution agreement through the National Research Council of Canada.

[1] S. Fartoukh – private communication

ISBN: 978-3-95450-184-7 doi:10.18429/JACoW-IPAC2018-TUPAL064

the nominal WP i.e. fractional tunes (0.31,0.32). At intensity $N_b = 1.1 \times 10^{11}$ p/b, both lattices show very similar dependence of DA on tune – Fig. 2, top. Here there are in fact 19 curves, each corresponding to the x-y angle shown in the legend, but spaces (stripes) between individual curves are colored with hue proportional to angle value (unavoidable overlap ignored). The locations of dips and maxima seen on Fig. 2 are discussed next.

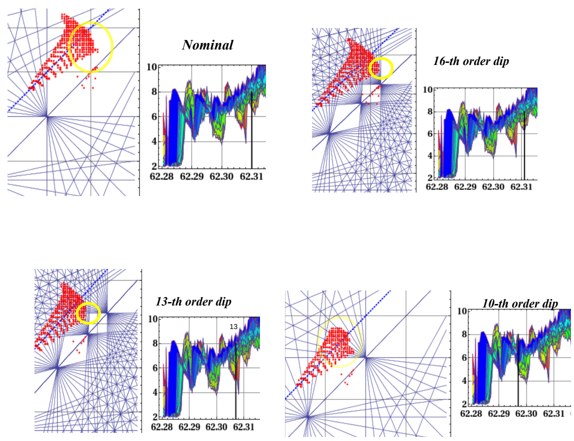

Figure 3: Left plots: beam-beam footprint with eliminated particles lost in 10^6 turns. Right plots: corresponding tune points on Fig. 2 (vertical black lines).

Dips in DA

For most of the plot on Fig. 2 the dips in minimum DA are well described by the red stripe, i.e. particles launched near the horizontal plane. These dips are created when the footprint's horizontal wing penetrates domain of denser resonances near the diagonal (yellow on Fig. 1) as clearly seen in Fig. 3) which shows the "surviving" part of the footprint at four locations: near the nominal WP 0.31 and near three of the dips caused by 16, 13 and 10-th order resonances. The effect of 16th order resonances is apparent from the top two plots of Fig. 3.

An analytic model [13], [14] was used to create the curves in blue on Fig. 2 (bottom). This model assumes presence of only two head-on collisions IP1 and IP5 to produce an analytic expression for the beam-beam invariant (first order ellipse distortion). The amplitude of some high-order harmonic of this invariant is plotted in blue. It's peaks are seen to agree well the locations of dips indicating that the corresponding resonances are driven by head-on collisions, while (in absence of octupoles) the role of long-ranges is solely to supply/generate the wing. Notice also that, as found in the above papers, of the two peaks near 62.31, the one at 62+4/13 depends on the tune advance between IP1 and IP5 and thus can be canceled if it is set to 1/4 × integer, while the other one at 62+5/16 is independent on this phase.

Optimum Tunes

Regarding the optimum DA locations, observe first that in terms of unperturbed $Q^0_{x,y}$ a tune-scan made with some lattice setup A should also predict optimum tunes for setup B of different ΔQ_x^{BB}. This is because the footprint's head scans the same resonance mesh at a distance equal to the difference between the tune-shifts of B and A. One can imagine that the horizontal wing scans the resonances as a "δ-function" so, to accuracy to translation along the abscissa, different tune-scans predict the same optima.

The above "projected" optima were used to construct Table 1. Here the previous HL-LHC scan of Fig. 2 is denoted as **case 0** and projected locations for two other HL-LHC setups are shown, with tune shifts ~ 0.2 (**case 1**) and ~ 0.3 (**case 2**). For example, in **case 1** the projected tune is $Q^0_x = 62.31 - (0.022 - 0.0155) = 62.3035$. Fig 4 demonstrates that cases **1** and **2** fall remarkably well near optimum locations.

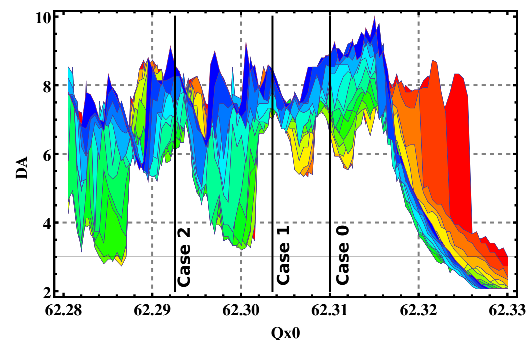

Figure 4: Same as on Fig. 2 top (left), but with vertical lines indicating "projected tune" cases of Table 1. Here the vertical axis, showing DA[σ], is only valid for **case 0**.

Table 1: Projected Q^0_x – black vertical lines on Fig 4

	HL-LHC setup (N_b in p/b)	tune shift	Q^0_x
0	as scan made: 1.1×10^{11}	0.0155	62.31
1	2.2×10^{11}, no BB in IP8	0.022	62.3035
2	2.2×10^{11} , with BB in IP8	0.033	62.2925

Finally, Figure 5 shows results from similar DA scans performed with the true lattice for cases **1** and **2**. Observe that on these plots the two regions near 62.31 locally look the same as the ones near corresponding projected tunes in Fig. 4.

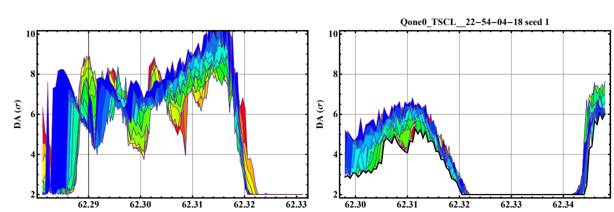

Figure 5: Tune scans with parameters as cases 1 and 2.

In summary, the linear tune-scans indicate that further improvement in DA should be sought if two dimensions, where most promising looks the region near the one-third corner (~0.32-0.33), and also that Landau octupoles should

ISBN: 978-3-95450-184-7 doi:10.18429/JACoW-IPAC2018-TUPAL064

be turned on, thereby reducing the transverse size of the the footprint (wings). Such features, along with higher chromaticity, have already been reported and included in recent HL-LHC lattices.

TWO-DIMENSIONAL SCANS

Strong Octupoles and High Chromaticity

In this section DA is evaluated over 2D domains and for HL-LHC parameters as in the baseline scenario, whose latest review can be found in [11], [12]. The contour plots represent minimum value of DA[σ] over 19 angles with σ as in the legend, shown on top of resonance lines of orders 5 to 16.

For Figures 6 and 7 we have taken some hypothetical (most pessimistic) case of doubling the intensity at a constant $\boldsymbol{\beta}^{\star}$: from $N_b = 1.1 \times 10^{11}$ shown on the left, to twice this value (on the right). In Fig 6, the chromaticity and Landau octupole current are as in the previous section. In Fig 7, $\boldsymbol{Q}' = 15$ and the maximum $|\boldsymbol{I}_{\mathbf{MO}}|$ is taken using the negative polarity. As independently found in [2], a region exists where he minimum DA exceeds $6\,\sigma$ in all four cases. The same is seen to be true for the sample leveling scenario on Figure 8.

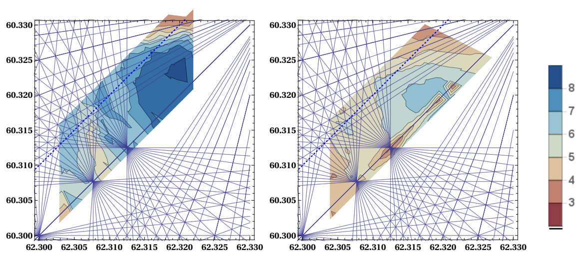

Figure 6: Left to right: doubling the intensity at constant $\boldsymbol{\beta}^{\star}$=15 cm (not a leveling scenario) for $\boldsymbol{Q}'$= 3, $\boldsymbol{I}_{\mathbf{MO}} = \mathbf{0}$.

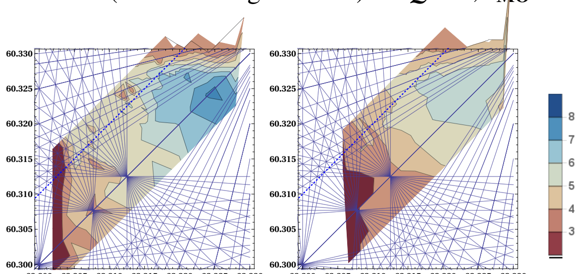

Figure 7: Left to right: doubling the intensity at constant $\boldsymbol{\beta}^{\star}$=20 cm (not a leveling scenario) for $\boldsymbol{Q}'$= 15, $\boldsymbol{I}_{\mathbf{MO}}$ = −570 A.

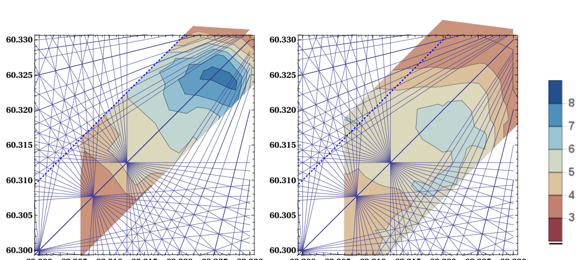

Figure 8: Some example leveling scenario for $\boldsymbol{Q}'$= 15, $\boldsymbol{I}_{\mathbf{MO}}$ =-570 A. Left: $\beta^{\star}$=46cm, $N_b = 2.2\ 10^{11}$ (beginning of fill). Right: $\beta^{\star}$=15cm, $N_b = 1.2\ 10^{11}$ (end of fill).

The left-side plots show that with chromaticity increased, the optimum tune domain exhibits a shift downwards and below the split-2 diagonal, a property first established in two-dimensional tune-scans performed previously for the LHC. A shift of the optimum tunes with intensity is also seen to take place, its exact value being somewhat obscured by the large scanning step used in all plots on the right, i.e. for doubled intensity.

Alternative Working Point

On Figure 9, the TS conditions are identical to the end-of-fill case above, Fig. 8 (right), but the scanning region has been extended to the left – away from the one-third corner, and also the steps are smaller: $\Delta Q^{\|\text{diag.}} = 5\ 10^{-4}$, $\Delta Q^{\perp\text{diag.}} = 4\ 10^{-3}$. Zoom of the region near the nominal tune allows to see the same resonances as in the previous section appearing here as contours transverse to the diagonal.

A new interesting region is also seen on Figure 9 near (62.3,60.3), i.e. in vicinity of 10th order resonance cluster, its 1D analogue can be found on Figure 3 (bottom, right). In this region the minimum DA over angles is at its peak larger by 1-1.5 σ than its corresponding value near the one-third corner, but the domain of good tunes (in blue) seems substantially reduced.

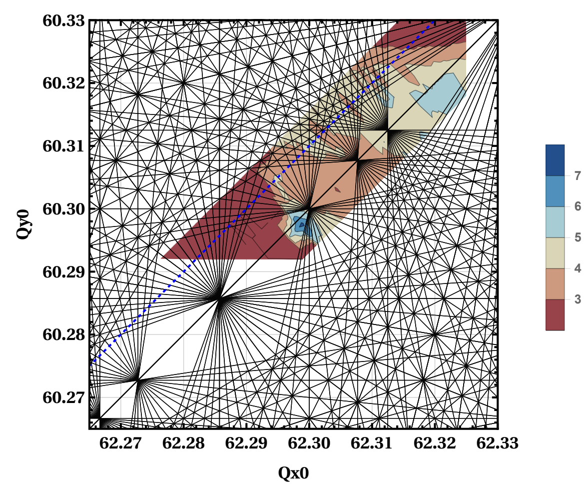

Figure 9: Same conditions as for Fig. 8 (right), but with tune-scan domain extended to the left, allowing to see a new region of large DA near (62.3,60.3).

REFERENCES

[1] G. Apollinari et al. eds. *High-Luminosity Large Hadron Collider Preliminary Design Report*, Journal of Instrumentation, Volume 11, Dec. 2016, `https://cds.cern.ch/record/2116337/files/CERN-2015-005.pdf`, CERN-2015-005.

[2] N. Karastathis *et al.*, “Refining the HL-LHC Operational Settings with Inputs From Dynamic Aperture (DA) Simulations: A Progress Report”, presented at IPAC’18. Vancouver, April-May 2018.

[3] D. Pellegrini, S. Fartoukh, N. Karastathis and Y. Papaphilippou, “Multiparametric response of the HL-LHC Dynamic Aperture in presence of beam-beam effects”, in *Proc. IPAC*

ISBN: 978-3-95450-184-7 doi:10.18429/JACoW-IPAC2018-TUPAL064

2017, Copenhagen, May 14-19, also in J. Phys. Conf. Ser. **874**, no. 1, 012007 (2017).

[4] Barranco J. *et al*., "LHC@Home: a BOINC-based volunteer computing infrastructure for physics studies at CERN", Open Eng. 7 (2017) 378-392

[5] W. Herr, E. McIntosh, F. Schmidt, D. Kaltchev, " Large Scale Beam-beam Simulations for the CERN LHC Using Distributed Computing", in *Proc. EPAC'06*, Edinburgh, UK, June 2006, paper MOPLS001, http://accelconf.web.cern.ch/AccelConf/e06/PAPERS/MOPLS001.PDF.

[6] A. Valishev *et al.*, "Preliminary estimates of beam-beam effects", HiLumi LHC Milestone report CERN-ACC-2014-0066, CERN, Geneva Switzerland (2014).

[7] D. Banfi, J. B. Garcia, T. Pieloni, A. Valishev, "Weak-strong Beam-beam Simulations for HL-LHC", in *Proc.of IPAC2014*, Dresden, Germany, June 2014.

[8] Grote H. and Schmidt F., 2016 MAD-X User's Guide, http://madx.web.cern.ch/madx/

[9] Schmidt F., *2012 SixTrack User Manual*, http://sixtrack.web.cern.ch/SixTrack/

[10] McIntosh E. and De Maria R. *2013 SixDesk User Manual* http://sixtrack.web.cern.ch/SixTrack/

[11] *High-Luminosity Large Hadron Collider (HL-LHC) technical design report V0*, edited by Apollinari, G, Béjar, Alonso I, Brüning O., Lamont M. and Rossi L, unpublished https://edms.cern.ch/ui/file/1558149

[12] Medina L. *et al*, in *Proceedings of IPAC2017*, Copenhagen, Denmark, May 2017, paper TUPIK089.

[13] Dobrin Kaltchev, "On beam-beam resonances observed in LHC tracking", TRIUMPH Report TRI-DN-07-9, 2007, http://beam01.triumf.ca/papers/pub/TRI-DN-07-9.pdf.

[14] W. Herr, D. Kaltchev, *Effect of phase advance between interaction points in the LHC on the beam-beam interactions*, http://doc.cern.ch/archive/electronic/cern/preprints/lhc/lhc-project-report-1082.pdfLHC Project Report 1082, 2008.